AD-Vol. 27

FRACTURE AND DAMAGE

edited by
A. NAGAR

FRACTURE AND DAMAGE

presented at
THE WINTER ANNUAL MEETING OF
THE AMERICAN SOCIETY OF MECHANICAL ENGINEERS
ANAHEIM, CALIFORNIA
NOVEMBER 8–13, 1992

sponsored by
THE AEROSPACE DIVISION, ASME

edited by
ARVIND NAGAR
WRIGHT LABORATORY

THE AMERICAN SOCIETY OF MECHANICAL ENGINEERS
345 East 47th Street ☐ United Engineering Center ☐ New York, N.Y. 10017

ISBN No. 0-7918-1074-7

Library of Congress
Catalog Number 92-56537

FOREWORD

One of the most significant technological advancements of this century has been to account for the local concentration and intensity of stresses around flaws and their effects on design, performance and maintenance of modern structures. The development of flaws in their various forms result from material processing, manufacturing practices, environment and in-service operating conditions. The damage due to the presence of initial flaws, if not controlled from further growth, often leads to a premature failure which is not predictable from overall material behavior.

The structures and materials in aerospace applications are subjected to complex cyclic loading and extreme environmental conditions including high temperatures. With pre-existing flaws, they offer limited resistance to damage accumulation and failure. In conventional metallic structures, the discontinuities and corroded surfaces have provided favorable conditions for crack initiation. In composites, the damage at the interfaces and at the regions affected by impact often initiates failure. The mechanics and mechanisms of fracture and damage for these applications have become critical areas of research and in recent years, the developments in these areas have been rapid. A symposium was planned to bring together experts in various areas of fracture and damage to exchange their results and observations. It was held on November 9–10 during the 1992 ASME Winter Annual Meeting. The symposium was sponsored by the Structures and Materials Technical Committee of the Aerospace Division of The American Society of Mechanical Engineers. Three sessions, two on modeling and analysis of fracture and damage, and one on modeling and experiments, were organized and presented.

This ASME volume contains papers presented at these sessions. Most papers deal with the mechanics of fracture and damage at elevated temperatures. The subject discussed here is not limited to a single material system or a class of material. Thus, this work brings some of the latest developments in the area of fracture and damage in a single volume. In particular, modeling, analysis and experimental techniques for interface damage in composites including the effects of residual stresses and temperatures; and crack growth, inelastic deformation and fracture parameters for isotropic materials are discussed.

In the first paper, Valanis discusses a local damage theory and shows a close agreement with the linear elastic fracture mechanics when the numerical analysis uses a particular finite element size called a "characteristic size." The unified view on fracture and damage is substantiated by experimental data on fracture stress. In the following paper, Kuo et al. present an integral formulation of a new parameter for time dependent crack growth at elevated temperatures and variable load conditions. For small scale creep conditions, this parameter is similar to C_t and the two differ only by a proportionality constant. Brust and Krishnaswamy present results of a computational study of time dependent crack growth at elevated temperatures using various constitutive relations. In the next paper, Shivakumar reports 3-D stress intensity factor solutions for centrally cracked thin plates under anti-plane loading using a virtual crack closure technique. The specimen geometry simulates a crack near the lap splice joint of fuselage. Birman and Nagar use the principle of virtual work to derive crack tip stresses and strain energy for orthotropic laminates reinforced by thin tougher layers. A new p-version finite element formulation for analysis of cracked composite laminates is presented by Saha et al.

In the area of fracture and damage modeling and analysis in composites, Reifsnider et al. discuss concepts for prediction of creep rupture strength and fracture in composites at elevated temperatures and present a life prediction model for the effects of residual stresses, creep deformation and activation processes. Sherwood et al. discuss thermomechanical behavior of titanium matrix composites with thermal residual stresses. The effects of interface damage (chemical bonding loss) is significant when applied strain is normal to the direction of fibers. A methodology to simulate the evolution of discrete damage at the fiber matrix interface is proposed. Santhosh et al. discuss a model to predict stress strain response of fiber reinforced metal matrix composites with fiber matrix debonding under elevated temperatures. Newaj and Majumdar report results of a study on deformation mechanisms in titanium matrix composites at elevated temperatures under pure compressive loads. Mohan presents computational aspects of modeling plasticity in crystalline solids from finite element view-point. A geometrically rigorous formulation of crystalline plasticity is adopted. The predictive capability of numerical simulations is compared with the experimental results.

The remaining five papers deal with damage modeling and experiments at elevated temperatures. Chu et al. present a theoretical model for ceramics with microcrack damage due to thermal shock by correlating elastic properties with microstructural degradaton. The model is verified using two independent experimental measurement techniques on alumina and silicon nitride. Delale et al. use interfacial strain energy release rate to describe monotonic stress-strain tensile behavior of ceramic matrix composites under occuring damage. Pernot el al. report that crack growth retardation occurs during sustained load at maximum in titanium aluminides. The experimental data was successfully correlated with a linear damage summation model when modified by a blunting coefficient. Harper and Sura discuss a model for nonlinear power law, transient creep in polyimide films. The results show that the time, temperature and stress superposition is applicable. Liu and Smith report experimental results for local stress strain, stable crack growth and fracture in highly filled polymeric materials.

The editor is indebted to the Air Force Wright Laboratory, Flight Dynamics Directorate for providing the support and encouragement to organize a symposium on fracture and damage and the opportunity to publish this volume. The assistance of Jalees Ahmad, AdTech Systems Research Corporation to solicit papers for the session on high temperature composites-modeling and analysis is appreciated. Victor Birman, University of Missouri-Rolla, helped to review the papers for the session in the area of modeling and experiments.

Sincere thanks are also due to Ozden Ochoa, Texas A&M University, for acquiring sessions for this symposium, for coordinating various activities for the symposium, and the timely publication of this ASME volume. Special thanks are also due to the staff of the ASME Technical Publishing Department for their cooperation.

Arvind Nagar

CONTENTS

AD-Vol. 27, Fracture and Damage
ASME 1992

SOME RECENT DEVELOPMENTS IN CONTINUUM DAMAGE THEORY

K. C. Valanis
Endochronics Incorporated
Vancouver, Washington
and
University of Portland
Portland, Oregon

ABSTRACT

In this paper we address a number of questions associated with local and non-local damage theories. The limitations of local theories are pointed out. Yet we show that the local theory proposed previously by the author [1] has certain utility when a 'characteristic' element size, which is defined, is used in the computations. Its physical validity is put to the test in the solution of the problem of a plate under tension with a central crack, at various angles to the direction of pull. The fracture stress, as a function of the crack length or inclination angle is compared with experimental data on grey cast iron. The agreement is excellent.

The non-local theory, also previously proposed by the author [2], is briefly introduced and discussed in the context of the initial value problem, which, in the case of the non-local theory, is hyperbolic but not so according to the local theory. Two numerical solutions [3] (one local and one non-local), to the initial value problem of a semi-infinite elastic rod, subject to a step velocity at one end, are discussed. The non-local solution converges to a physically realistic limit, while the local solution degenerates to a null solution as the grid size tends to zero.

INTRODUCTION

During the last decade we have witnessed the rise of continuum damage theory to a level of analytical sophistication. See typically Refs. [4-31]. With the exception of some recent papers, these theories are of the "local" type in the sense that damage in a neighborhood is a function of the history of the mechanical state of that neighborhood. As was discussed in a previous article [4], the difficulty with local theories is that in the softening regime *i.e.*, when:

$$d\sigma_{ij}\, d\varepsilon_{ij} \leq 0 \tag{1}$$

the governing equation of the initial value problem is no longer hyperbolic and uniqueness of the solution cannot be proved. A similar situation arises in the case of the boundary value problem.

When a numerical solution is attempted in terms of a finite element scheme, it transpires that the solution is excessively sensitive to the element size and gives rise to physically unrealistic predictions as the element size tends to zero. To remedy the problem we [2] introduced a non-local damage theory where the damage process of a material neighborhood is influenced by the entire strain field of the material domain. To demonstrate the differences between the two theories, an axial wave propagation problem was solved by Murakami, Kendall and Valanis [3], using a finite element technique. The problem was that of a semi-infinite rod, initially at rest, to which a step velocity of - 0.6 m/s was applied at one end. It was found that the 'local' solution, in terms of the particle velocity history at a point along the rod, degenerates to a null solution as the element size goes to zero. On the other hand, the 'non-local' solution converges to a physically realistic limit. See Figs. 1 and 2.

However, another item of interest was observed as a result of the analysis. When a particular finite element size, a characteristic size, was used in the numerical analysis in conjunction with the local theory, the solution was not far from that obtained by the non-local theory. On the basis of the local theory alone, the physical meaning of the characteristic size is not clear, but it acquires a clear meaning in the context of the non-local theory. This question will be taken up again in the section on the non-local theory and its relevance to the application of the local theory to the numerical determination of the fracture stress of a thin cast iron plate with a central sharp crack inclined at various angles to the direction of pull.

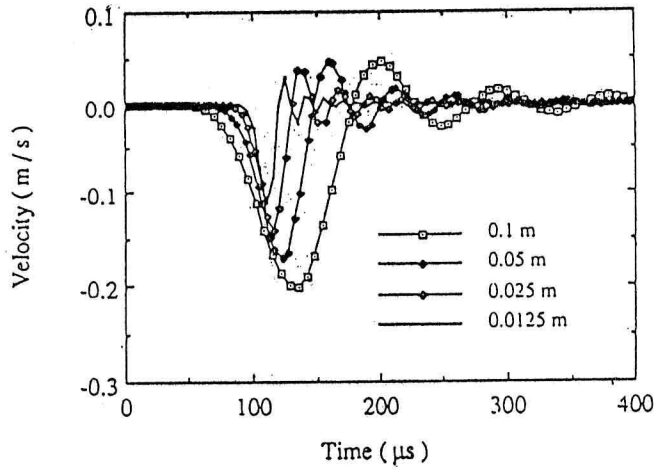

Figure 1. Velocity history at distance 0.4 m from end of semi-infinite rod (local solution).

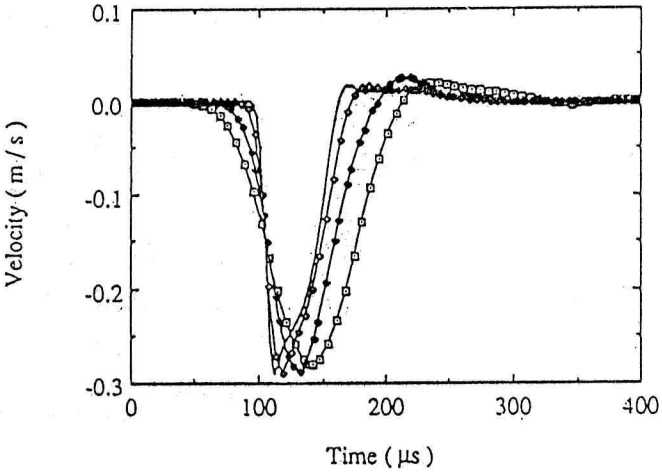

Figure 2. Velocity history at distance 0.4 m from end of semi-infinite rod (non-local solution).

This problem is critical in proving the worth of continuum damage theories because often, fracture occurs by the extension of one dominant crack, in the presence of distributed damage. Hence, a damage theory, must deal with the presence of sharp cracks. Also Linear Fracture Mechanics (LEFM) can deal successfully with fracture due to sharp cracks in Mode I conditions. A continuum damage theory, therefore, should have a common boundary with LEFM. That the present local theory has that property has now been demonstrated. It and LEFM, give values of fracture stress that are in close agreement between themselves and those determined experimentally. Evidently the grid size chosen in the local analysis had the 'characteristic' size.

LOCAL DAMAGE THEORY

The basic premise of the theory is that directed damage may be represented by a tensor valued function $\underset{\sim}{\phi}$, "the integrity tensor", which appears explicitly in the equation for the free energy and the constitutive equation. Thermodynamically, $\underset{\sim}{\phi}$ is an internal variable. In linear elastic-fracturing solids, the free energy density is given by Eq. (2a) and the constitutive relation by Eq. (2c), where λ and μ are the Lamé constants.

$$\psi = (\lambda / 2)\phi_{ij}\phi_{kl}\varepsilon_{ij}\varepsilon_{kl} + \mu\phi_{ik}\phi_{jl}\varepsilon_{ij}\varepsilon_{kl} \tag{2a}$$

Thus, since:

$$\underset{\sim}{\sigma} = \partial\psi / \partial\underset{\sim}{\varepsilon} \tag{2b}$$

it follows that:

$$\sigma_{ij} = \lambda\phi_{ij}\phi_{kl}\varepsilon_{kl} + 2\mu\phi_{ik}\phi_{jl}\varepsilon_{kl} \tag{2c}$$

Equation (2.1a) is a statement to the fact that:

$$\psi = 1/2\, C_{ijkl}\, \varepsilon_{ij}\, \varepsilon_{kl} \tag{2d}$$

where $\underset{\sim}{C}$, the stiffness tensor, is homogeneous and quadratic in $\underset{\sim}{\phi}$. There are two questions regarding $\underset{\sim}{\phi}$: How it is related to the material damage at some microscale and (ii) how it evolves with the history of deformation. In regard to question (i), it was previously shown, Valanis (1987), that if in a material element a principal values of $\underset{\sim}{\phi}$, say ϕ_r, is zero,, and $\vec{N}_r$ is the eigenvector of ϕ_r, the traction on a surface normal to $\vec{N}_r$ then is zero and the element cannot support traction on that surface. Thus, ϕ_r represents damage on a plane normal to $\vec{N}_r$, and as such it is a measure of the effective area in that plane. Hence, when $\phi_r = 0$, an effective plane crack has developed across the entire element on a plane normal to $\vec{N}_r$. Note that if $\phi_r = 1$ the damage on that plane is zero. In regard to question (ii) *i.e.*, the evolution of $\underset{\sim}{\phi}$, Eq. (3) was proposed:

$$d\phi^r = -\left(Q_n^r\right)^m d\xi^r \tag{3}$$

In the following notation: $d\phi^r$ is the change in principal component ϕ^r of $\underset{\sim}{\phi}$ and n_i^r are the eigenvectors of $d\underset{\sim}{\varepsilon}$; ξ^r is a damage coordinate and Q_n^r a "damage force" acting in the direction $\vec{n}$, *i.e.*,

$$Q_n^r = n_i^r n_j^r Q_{ij} \qquad (r, \text{ not summed}) \tag{4}$$

The damage coordinate, ξ_r is given by Eq. (5) *i.e.*,

$$d\xi_r = \begin{cases} k d\varepsilon^r\,;\, d\varepsilon^r > 0, & \varepsilon_n^r \geq 0, Q_n^r > 0. \\ 0, \text{ otherwise} \end{cases} \tag{5}$$

where $\varepsilon_n^r = \varepsilon_{ij} n_i^r n_j^r$ (r, not summed) and k is a positive scalar.

To determine $\underset{\sim}{Q}$ we appealed directly to thermodynamics. Since $\underset{\sim}{\phi}$ is an internal variable, the thermodynamic force $\underset{\sim}{Q}$ that drives the damage process is given by the relation

$$\underset{\sim}{Q} = -\partial\psi / \partial \underset{\sim}{\phi} \tag{6}$$

We now reason as follows. The direction of the damage increment - $d\underset{\sim}{\phi}$ is dictated by the eigendirections $\vec{n}^\alpha$ of the increment of strain $d\underset{\sim}{\varepsilon}$. In other words $d\underset{\sim}{\phi}$ and $d\underset{\sim}{\varepsilon}$ are coaxial. The force driving the damage process in the direction $\vec{n}^\alpha$ is then Q_n^a, which is $\underset{\sim}{Q}$ projected in the direction $\vec{n}^\alpha$. Thus

$$Q_n^\alpha = n_i^\alpha n_j^\alpha Q_{ij} \qquad (\alpha \text{ not summed}) \tag{7}$$

It follows from thermodynamic principles that:

$$d\phi^\alpha / d\xi^\alpha = bQ_n^\alpha \tag{8}$$

where b is a material scalar and

$$d\xi^\alpha = \begin{cases} kd\varepsilon^\alpha \\ 0 \end{cases}, \quad d\xi^\alpha \geq 0, \tag{9}$$

k having the significance of a damage propensity parameter. But, the Clausius-Duhem dissipation inequality, *i.e.*,

$$-\frac{\partial\psi}{\partial\underset{\sim}{\phi}} \bullet d\underset{\sim}{\phi} > 0 \quad , \quad \left\| d\underset{\sim}{\phi} \right\| \neq 0 \tag{10}$$

must be observed. Thus in view of Eqs. (6) and (8) and the fact that

$$d\phi_{ij} = \sum_\alpha d\phi^\alpha n_i^\alpha n_j^\alpha \tag{11}$$

$\vec{n}^\alpha$ being eigenvectors of $d\underset{\sim}{\phi}$, it follows that

$$-\frac{\partial\psi}{\partial\underset{\sim}{\phi}} \bullet d\underset{\sim}{\phi} = -\sum_\alpha d\phi^\alpha \frac{\partial\psi}{\partial\phi_{ij}} n_i^\alpha n_j^\alpha > 0. \tag{12}$$

Since Ineq. (12) must be true for each α individually, *i.e..*, for each independent fracture mechanism, then the following inequalities must be satisfied for all α:

$$-d\phi^\alpha \frac{\partial\psi}{\partial\phi_{ij}} n_i^\alpha n_j^\alpha > 0 \quad ; \quad \left(\partial\psi/\partial\phi_{ij}\right) n_i^\alpha n_j^\alpha > 0 \tag{13,14}$$

for all α, whenever $|d\phi^\alpha| \neq 0$, since $d\phi^\alpha$ is negative when non-zero. We now have the full set of conditions that govern the evolution of the damage coordinate $d\xi^\alpha$. Thus:

$$d\xi^\alpha = kd\varepsilon^\alpha \tag{15}$$

whenever:

$$d\varepsilon^\alpha > 0 \quad , \quad \varepsilon_n^\alpha \geq 0 \quad , \quad \frac{\partial\psi}{\partial\phi_{ij}} n_i^\alpha n_j^\alpha > 0 \tag{16}$$

but $d\xi^\alpha = 0$ otherwise. We write Eq. (8) in its explicit form given below:

$$d\phi^\alpha = -bd\xi^\alpha \left(\lambda\varepsilon_{ij}(\phi_{kl}\varepsilon_{kl}) + 2\mu\phi_{kl}\varepsilon_{ik}\varepsilon_{jl}\right) n_i^\alpha n_j^\alpha \tag{17}$$

Material Parameters and Their Experimental Determination.

With b = 1, there are three constants to be determined: k, the fracture susceptibility and λ and μ. In a uniaxial test Young's modulus E was determined, while v was set equal to 0.3. Thus λ and μ were found to be 15 x 10^3 and 10 x 10^3 ksi, respectively. The constant k was determined from a simple tension test on an uncracked specimen. Under these conditions

$$\sigma_{1\max} = E(1/2keE)^{1/3} \tag{18}$$

where loge = 1. With σ_{1max} (experimental) = 40 ksi, k is 2 x 10^3 $(ksi)^{-1}$.

COMPUTATIONAL STUDY.

The computations consisted of developing a Finite Element Program and computing the deformation, stress and damage fields in a flat plate in with a central crack of various lengths. A grid of square elements was used, with each of unit length equation of 3/64 in. The domain was 16 units wide and 21 units long. Stress, strain and damage fields were obtained. Longitudinal displacement control (with free transverse displacement) on the outer boundary was used. All other boundaries were stress-free. An incremental displacement of 2.5 x 10^{-3} units was applied. The computations were performed on a VAX 750 computer. For details see Ref. [1].

Figure 3 shows the calculated curve of fracture stress versus crack length, when this varied in size from two elements to fourteen. Also shown, are the experimentally determined values of fracture stress on gray cast iron,. The experiments were carried out at the Materials Laboratory of the University of Portland and have been reported previously [16]. The comparison shows excellent agreement between calculated and experimental data.

Figure 4 shows the damage distribution along the crack line, when the half-crack is one unit long. The calculated damage away from the crack is indeed

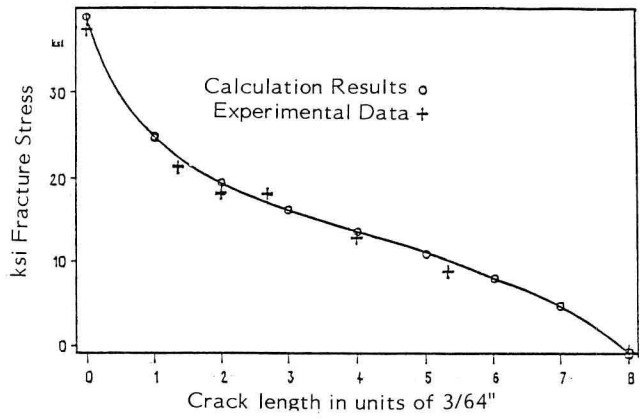

Figure 3. Calculated versus observed fracture stress (continuum damage theory).

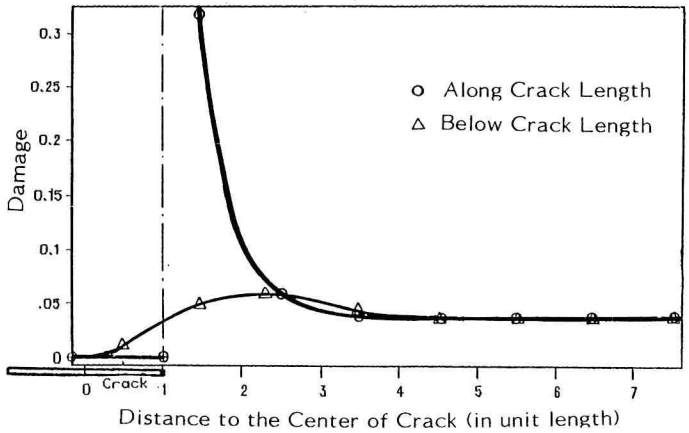

Figure 4. Damage distribution along and below crack line.

negligible. In Fig. 5 we show the predictions of LEFM against a backdrop of experimental values. Excellent agreement is again shown with the exception of very small cracks. Figure 6 is a comparison of the experimental and theoretical values of fracture stress, where these are functions of inclination of the crack to the direction of pull. Again agreement with experiment is close.

THE NON-LOCAL THEORY.

The theory was given in detail in a previous paper [2]. Here we give its essential features. The difference between the local and the non-local theory lies in the definition of the damage coordinate ξ_r. In the local theory $d\xi_r$ is given by Eq. (5) in conjunction with Eqs. (4) and (6). To reiterate,

$$d\xi_r = k\, n_i^r n_j^r\, d\varepsilon_{ij} \qquad (19)$$

provided that the attendant inequalities discussed previously are satisfied.

In the local theory we introduce a non-local strain increment field $d\varepsilon_{ij}^G$ where:

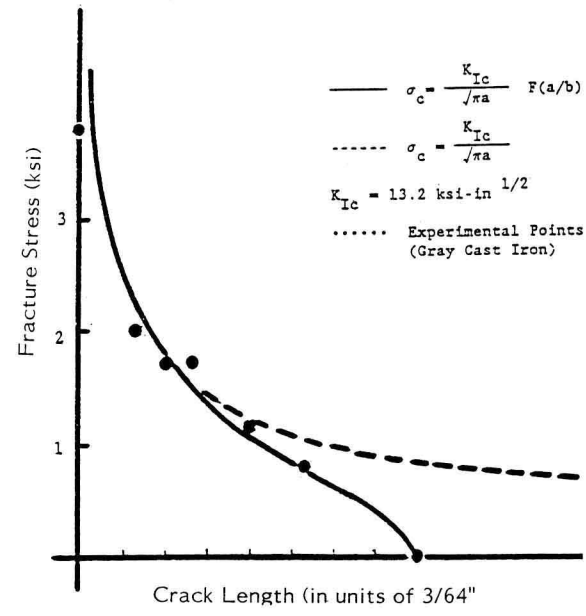

Figure 5. Comparison of LEFM prediction with experimental data.

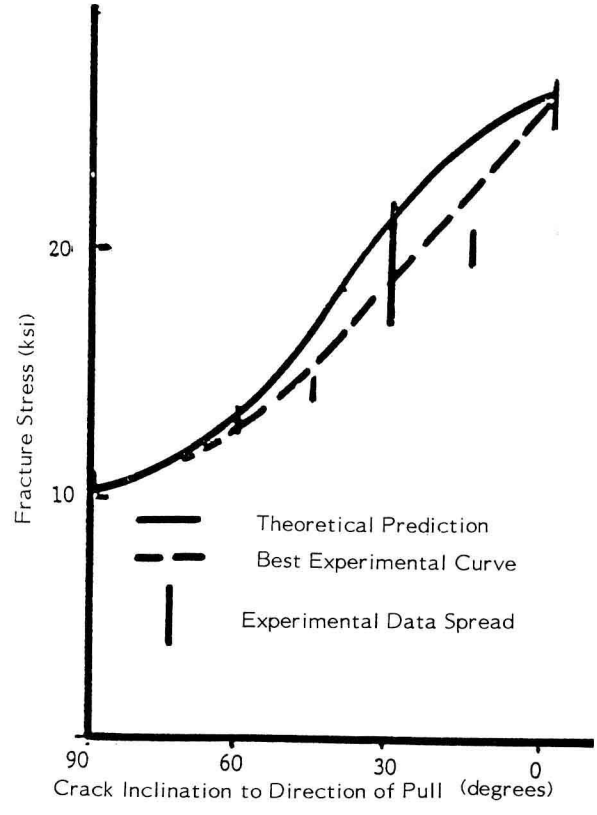

Figure 6. Fracture stress versus angle of crack inclination to direction of pull.

$$d\varepsilon_{ij}^{G} = \int_{V} k(x_i, x_i')\, d\varepsilon_{ij}(x_i')\, dV \qquad (20)$$

where $k(\cdot)$ is positive symmetric function in x_i and x'_i. We then introduce the global damage coordinate $d\xi_r^G(x_i)$ where at x_i:

$$d\xi_r^G = n_i^r n_j^r\, d\varepsilon_{ij}^G \qquad (21)$$

provided that $d\varepsilon_r > 0$, $\varepsilon_n^r \geq 0$ and $Q_n^r > 0$, otherwise $d\varepsilon_r^G = 0$. Then, if $d\xi_r^G > 0$,

$$d\xi_r = d\xi_r^G \qquad (22)$$

otherwise $d\xi_r = 0$.

Notice that, in the non-local theory, the constant k of the local theory has been replaced by the influence function $k(x_i, x'_i)$. For initially homogeneous materials:

$$k(x_i, x_i') = k(|x_i - x'i|) \qquad (23)$$

Thus the local theory is a degenerate case of the non-local theory when $k(x_i)$ is proportional to the Dirac delta function. Evidently $k(x_i)$ has a maximum at $x_i = 0$ and decays to zero as $|x_i| \to \infty$. The rate of decay is indicative of the non-locality of a material.

The normal distribution function is an evident candidate for $k(x)$. In this case:

$$k(x) = k_o \sqrt{b/\pi} \exp\left(-bx^2\right) \qquad (24)$$

Note that $k_o^{-1} \int_o^\infty k(x)dx = 1$ and $k(x)/k_o \to \delta(x)$ as $b \to \infty$.

In a three-dimensional domain, we set:

$$k(x_i - x_i') = k_o \{b/\pi\}^{3/2} \exp\left(-b\rho^2\right) \qquad (25)$$

where:

$$\rho^2 = \sum_i \left|(x_i - x_i')\right|^2 \qquad (26)$$

In a finite element analysis, where the stress and strain field in each individual element are uniform, the global strain tensor field increment is represented by the vector of the global strain increments in the individual elements. Thus if $d\underset{\sim}{\varepsilon}_\alpha^G$ is the global strain increment in element α then Eq. (20) reduces to the form:

$$d\underset{\sim\alpha}{\varepsilon}^G = k_{\alpha\beta}\, d\underset{\sim\beta}{\varepsilon} \qquad (27)$$

where $k_{\alpha\beta}$ is the influence matrix whose elements are determined from Eq. (20) in conjunction with Eq. (26). Thus, if in a material domain the mean distance between elements α and β is $\rho_{\alpha\beta}$ then, approximately,

$$k_{\alpha\beta} = \Delta V\, k_o \{b/\pi\}^{3/2} \exp\left\{-b^2 \rho_{\alpha\beta}\right\} \qquad (28)$$

presuming that the finite elements are equivoluminal. The error implicit in the calculation decreases as the root mean square dimension of the element tends to zero. Note that the values of components of $k_{\alpha\beta}$ depend on the size of the grid!!

Of great interest is the case where the root mean square dimension of the element is equal to the spread of the distribution, *i.e.*, when:

$$\Delta V = \{b/\pi\}^{3/2} \qquad (29)$$

Then, because the influence function decays rapidly with $\rho_{\alpha\beta}$, only the diagonal terms in $k_{\alpha\beta}$ are significant (as a first approximation). Hence:

$$d\underset{\sim\alpha}{\varepsilon}^G = k_o\, d\underset{\sim\alpha}{\varepsilon} \qquad (30)$$

Notably, the non-local theory reduces to the local form, but this is true only when the finite element size has a characteristic value defined by Eq. (29). Specifically one cannot vary the size of the finite element without the full matrix $k_{\alpha\beta}$ coming into play. Therefore, the accuracy of the solution by the local theory is limited by the characteristic size, which is fixed.

The above analysis explains the curious result obtained by Murakami, Kendall and Valanis [3] in the numerical solution of the wave propagation problem, discussed previously, where the local theory led to results that were close to those of the non-local theory, for a specific (but not knowable) size of the finite element grid! It also corroborates the validity of the finite element analysis of the plate with a central crack. The implication is that the finite element size chosen was in fact close to the characteristic size, which therefore may be determined by the solution to such a problem.

Remark.

We close this section by pointing out that the excessive dependence of the solution to the initial value problem on element size, cannot be remedied by letting the damage susceptibility parameter depend on the element size. Such dependence would lead to a loss of uniqueness of the solution to boundary value problem of a homogeneous domain under homogeneous tractions. In the absence of damage the solution to this problem by a finite element technique is exact, unique and independent of element size. However, in the presence of damage, different finite element sizes will give rise to different solutions in view of the size dependence of the susceptibility parameter.

EFFECT OF SIZE OF MATERIAL DOMAIN ON STRENGTH.

In the above section we discussed the effect of finite grid size on the character of the numerical solution. However there is another "size effect", that of the dependence of strength on the size of the material domain. For the sake of reference we shall call this the Domain Effect as opposed the grid size effect which we shall call the Grid Effect. It is of interest that the local theory does not predict the experimentally observed Domain Effect, when it should, and yet it gives rise to the Grid Effect when it should not.

One might argue around this difficulty by presuming that no material domain is entirely damage-free in its reference state, and introducing the Weibull "predominant crack theory" according to which fracture occurs as a result of a flaw, the expected size of which increases probabilistically with the size of the specimen. The fact is, however, that if a specimen is homogeneous and, hence, statistically uniform, a flaw is equally likely to occur anywhere in the specimen. If then fracture originates at the site of the largest flaw, then the fracture surface is equally likely to lie anywhere in the specimen. This is certainly not true in the case of fracture under axial tension in light of the experimental evidence that fracture occurs predominantly near the center of the specimen.

In contrast the non-local theory, quite correctly, provides insensitivity of the solution to grid size while it predicts the Domain Effect. This is because the increment in damage is proportional to the increment in the damage coordinate $d\xi$, which increases with the size of the material domain! The non-local theory also predicts fracture at the center of a specimen under uniform tensile strain as shown in Ref. [2].

Acknowledgement

The author acknowledges support by the Air Force Office of Scientific Research, Directorate of Aerospace Sciences, Civil Engineering Program, Bolling Air Force Base, Washington, D.C.

REFERENCES

[1] Valanis, K. C., 1990, "A Theory of Damage in Brittle Materials", *Eng. Fract. Mech.*, 36, 403-416.

[2] Valanis, K. C., 1991, "A Global Damage Theory and the Hyperbolicity of the Wave Problem", *J. A. Mech.*, 58, 311 - 318.

[3] Murakami, H., Kendall, D. M. and Valanis, K. C., "A Non-Local Elastic Damage Theory: Mesh Insensitivity Under Strain Softening", *Int. J. Comp. and Struct.* (Submitted)

[4] Valanis, K. C., 1985, "On the Uniqueness of Solution of the Initial Value Problem in Softening Materials", *J. A. Mech.*, 52, 649.

[5] Dragon, A., and Mroz, Z., 1979, "A Continuum Model for Plastic-Brittle Behavior of Rock and Concrete", *Int. J. Eng. Sci.*, 17, 121 - 137.

[6] Chaboche, J. L., 1979, "The Concept of Effective Stress Applied to Elasticity and Viscoelasticity in the Presence of Anisotropic Damage", Royal Aircraft Est., Report No. 1979-77, Farnborough.

[7] Krajcinovic, D., and Fouseka, G., 1981, "The Continuous Damage Theory of Brittle Materials, Part I", *J. App. Mech.*, 48, 809.

[8] Fouseka, G., and Krajcinovic, D., 1981, "The Continuous Damage Theory of Brittle Materials, Part II", *J. Appl. Mech.*, 48, 816.

[9] Lamaitre, J., and Lazars, J., 1982, "Application de la Theorie de L'Endommagement au Comportement Nonlineaire at la Rurture du Beton de Structure", *Annales de I' ITBTP*, 41.

[10] Bazant, Z., Belystschko, T., and Chang, T., 1984, "Continuum Theory of Strain Softening", *J. Eng. Mech. Div., ASCE*, 110, 1666.

[11] Krajcinovic, D., and Fanella, D., 1986, "A Micromechanical Damage Model for Concrete", *Eng Fract. Mech.*, 25, 385 - 396.

[12] Bazant A., and Belystschko, T., 1987, "Strain Softening Continuum Damage: Localization and Size Effects", Proc. Intl. Confr. on Constitutive Laws for Engr. Matls., Vol. 1, C. S. Desai *et al*, Ed., Tuscon, AR, Elsevier, NY.

[13] Chaboche, J. L., 1988, "Continuum Damage Mechanics, Part I - General Concepts; Part II - Damage Growth, Crack Initiation and Crack Growth", *J. App. Mech.*, 55, 59 - 72.

[14] Valanis, K. C., 1987, "A Continuous Damage Model for Concrete", In Development of Advanced Constitutive Models for Plain and Reinforced Concrete, by Hegemier, G., Read, H., Valanis, K. C., and Murakami, H., S-Cubed Report SSS-R-87-8454.

[15] Valanis, K. C., 1989, "Continuum Modelling of Damage Due to Sharp Cracks", Proceedings, PLASTICITY 89: The 2nd Symposium on Plasticity and its Current Applications, Mie University.

[16] Valanis, K. C., 1988, "A Theory of Damage in Brittle and Semi-Brittle Materials", ENDOCHRONICS Report ENDIC-005-AFOSR-1988.

[17] Valanis, K. C., 1989, "A Theory of Damage in Brittle and Cementitious Materials", ENDOCHRONICS Report ENDIC-007-AFOSR-1989.

[18] Read, H. E., and Hegemier, G. A., 1984, "Strain Softening of Rock, Soil and Concrete - A Review Article", *Mechanics of Materials*, 3, 271.

[19] Hegemier, G. A., and Read, H. E., 1985, "On Deformation and Failure of Brittle Solids: Some Outstanding Issues", *Mechanics of Materials*, 4, 215.

[20] Sandler, I. S., 1984, "Static Softening for Static and Dynamic Problems", ASME Symposium on Computational Aspects of Strain Softening.

[21] Murakami, H., Kendall, D. M., and Valanis, K. C., 1991, "Numerical Validation of a Non-Local Damage Theory", Constitutive Laws for Engineering Materials., Eds. C. S. Desai, *et al*, pp. 743 - 746.

[22] Triantafyllides, N., and Aifantis, E. C., 1986, "A Gradient Approach to the Localization of Deformation, I Hyperelastic Materials", *Jr. of Elasticity*, 16, 225 - 237.

[23] Cedolin, L., and Bazant, Z. P., 1981, "Fracture Mechanics of Crack Bands in Concrete", Fracture

Mechanics Methods for Ceramics, Rocks and Concrete, Eds. S. W. Freiman and E. P. Fuller, Am. Soc. for Testing Materials STP 745, pp. 87 - 95.

[24] Bazant, Z. P., 1984, "Size Effect in Blunt Fracture: Concrete, Rock and Metal", *J. Eng. Mech, ASCE*, 110, 518 - 535.

[25] Bazant, Z. P., Belystschko, T. B., and Chang, T. P., 1984, "Continuum Theory for Strain Softening", *J. Eng. Mech. ASCE*, 110, 1666 - 1692.

[26] Bazant, Z. P., 1991, "Recent Progress in Damage Modeling: Non-Locality and its Microstructure", Constitutive Laws for Engineering Materials, Eds., Desai, C. S., *et al.*, pp. 277 - 285, ASME Press.

[27] Bazant, Z., P., and Pijaudier-Cabot, G., 1989, "Non-Local Continuum Damage, Localization, Instability and Convergence", *J. App. Mech.*, 55, 287 0- 293.

[28] Valanis, K. C., 1990, "On the Non-Locality of the Damage Process", Invited Lecture, MINISYMPOSIUM on Theoretical, Experimental and Computational Problems Related to Rock and Concrete - Dean Norman, Waterways Experiment Station.

[29] Ortiz, M., 1985, "A Constitutive Theory for the Inelastic Behavior of Concrete", *Mechanics of Materials*, 4, 67.

[30] Yazdani, S., and Schreyer, H. L., 1988, "An Anisotropic Damage Model with Dilatation for Concrete", *Mechanics of Materials*, 7, 231.

[31] Yazdani, S., and Schreyer, H. L., 1990, "Combined Plasticity and Damage Mechanics Model for Concrete" *J. Eng. Mech.*, 116, 1435.

MODELING OF TIME DEPENDENT FRACTURE UNDER ELEVATED TEMPERATURES

An-Yu Kuo and Kuan-Luen Chen
Structural Integrity Assoc., Inc.
San Jose, California

Ashok Saxena
Mechanical Properties Research Lab.
Georgia Institute of Technology
Atlanta, Georgia

Arvind Nagar
Flight Dynamics Directorate (WL/FIBE)
Wright-Patterson AFB, Ohio

ABSTRACT

C_t has been found to be an effective parameter to characterize steady-state and transient creep crack growth rates. An integral formulation for computing C_t numerically is proposed in this paper, which complements existing C_t formulation used in laboratory measurements.

INTRODUCTION

The C_t parameter defined by Saxena [1] is a generalization of C^* but is different from the C(t)-Integral [2]. C_t generalizes upon the energy rate interpretation of C^* as follows. Consider several identical pairs of cracked specimens. Within each pair, one specimen has a crack length a and the other has an incrementally larger crack length a + Δa. The specimen of each pair are loaded to various constant load levels P_1, P_2, P_3, . . . P_i, etc. at elevated temperatures, and the load-line deflection as a function of time is recorded (Figure 1a). The load-line deflection due to creep is V_c. It is assumed that no crack extension occurs in any of the specimens and the instantaneous response is linear elastic. At a fixed time, the load versus deflection rate, $\dot{V}_c$, behavior is plotted for all specimens. A schematic of the expected behavior is shown in Figure 1b. Several such plots can be generated from these tests by varying time.

The area between the P-$\dot{V}_c$ curves for specimens with crack length a and a + Δa, is called ΔU_t^* (the subscript denotes that this value is at a fixed time, t). The C_t parameter is given by the following equation,

$$C_t = -\frac{1}{B}\frac{\partial U_t^*}{\partial a} \qquad (1)$$

where, B is specimen thickness. As $t \to \infty$, $C_t = C^*$ by definition because $\partial U_t^* / \partial a = dU^*/da$ under steady-state conditions.

C_t can be measured at the loading pins and can also be calculated as will be discussed later. It has also been shown to be directly related to the rate of expansion of the creep zone size in the small scale creep region [3] and it may then be argued that the rate of crack tip damage accumulation must scale with the rate of creep zone expansion. Thus, C_t can be expected to characterize the creep crack growth rate in the small-scale creep and the transition creep region. This has been borne out by a considerable amount of data [4].

As discussed in Reference 5, C_t appears to be the best parameter, among C_t, C(t), K and C^*, for characterizing creep crack growth of titanium intermetallics under transient as well as steady-state creep. The same behavior for steel has been reported by Saxena and his co-workers (see e.g., [3]) in their experimental results. The good correlation between C_t and creep crack growth can be attributed to the fact that C_t is proportional to the rate of expansion of the creep zone [3], which characterizes the damage zone at the crack tip region under creep conditions.

Although both C_t and C(t) are related to the crack tip damage (or stress) under creep conditions, C_t can be readily measured from load line deflection curves in a test while C(t) can only be computed. On the other hand, C(t) is easier to compute than C_t for structural components. This paper reexamines the definition of C_t and provides a line integral formulation for C_t as well as alternative ways of computing C_t.

PSEUDO-POTENTIAL P^* AND C_o

For a two-dimensional structure, we define pseudo-potential P^* as

$$P^* = \int_{\partial A_t} T_i \dot{u}_i \, ds - \int_A W^* \, dA \qquad (2)$$

where A is the entire body, ∂A_t is the boundary of A on which traction is specified, and W^* is defined by

$$W^* = \int_0^{\dot{e}_{ij}} \sigma_{kl}\, d\dot{e}_{kl} \qquad (3)$$

It is worth noting that, even though the expression of W^* in equation (2) looks simple and somewhat familiar, W^* does not bear any physical meaning. The first term in equation (2), which is the total power which flows into the body at a given instant, depends only on the current state (stresses, strains, and strain rates) of the body. On the contrary, the second term in equation (2) is history dependent. In other words, for a structure body A, the first part of P^* is a function of its current state while the second part of P^* depends on the loading path from time zero.

For a stationary crack, we then define another quantity $C_o(t)$ as

$$C_o(t) = \frac{dP^*}{da} = \frac{d}{da}\left[\int_{\partial A_t} T_i\, \dot{u}_i\, ds - \int_A W^*\, dA\right] \qquad (4)$$

where a is the crack length. It will be shown later in this paper that C_o and C_t are uniquely related in small scale creep and steady-state creep conditions. It should be noted that A in equation (4) is the entire body and equation (4) is defined for two stationary cracks at length of a and a+Δa under the same loading conditions. The subscript "o" of C_o stands for the outer boundary. By following the same procedure as that used by Rice [6] in deriving the well-known J-integral, it can be shown that equation (4) can be reduced to

$$\begin{aligned} C_o(t) &= \int_{\partial A} (W^*\, n_1 - T_i\, \dot{u}_{i,1})\, ds - \int_A (W^*_{,a} - \sigma_{ij}\, \dot{e}_{ij,a})\, dA \\ &= C(t)|_{\partial A} - \int_A (W^*_{,a} - \sigma_{ij}\, \dot{e}_{ij,a})\, dA \end{aligned} \qquad (5)$$

where A is the whole structure body and ∂A is the entire outer boundary of the body. Thus, the new parameter C_o defined in equation (4) is nothing but an area integral plus the C(t) integral [2] computed along the outer boundary of the body. The area integral in equation (5), however, is not always zero since, in general, W^* is a function of $\dot{e}_{ij}$, σ_{ij}, . . ., implying $W^*_{,a} \neq \sigma_{ij}\dot{e}_{ij,a}$. The inequality of C_o and C(t) has also been observed numerically by Bassani, et al, [3] and Leung, et al, [7]. Further, like C_t and C(t), $C_o(t)$, in general, is not path independent.

STEADY-STATE CREEP

From equation (5), it can be easily deduced that, at large times $t \to \infty$,

$$C_o(t) = C_t(t) = C(t) = C^* = \int_\Gamma (W^*\, n_1 - T_i\, \dot{u}_{i,1})\, ds \qquad (6)$$

where Γ is any integration contour which encompasses the crack tip counterclockwise since

$$W^* = W^*(\dot{e}_{ij}) \qquad (7)$$

$$W^*_{,a} = (\partial W^* / \partial \dot{e}_{ij})\dot{e}_{ij,a} = \sigma_{ij}\, \dot{e}_{ij,a} \qquad (8)$$

is true under steady-state creep conditions. Therefore, for steady-state creep, C^*, C(t), C_o and C_t all represent the same physical quantity.

SMALL SCALE CREEP

We next examine the behavior of C_o at the other end of the time spectrum, very small times $t \to 0$. As illustrated in Figure 2, when the elapsed time t is much less than the transition-time t_T defined by

$$t_T = K^2 (1-\nu^2) / [E(n+1)c^*] \qquad (9)$$

the creep dominant zone A_c' is much smaller than the surrounding elastic zone A_e. The creep dominant zone A_c' has the same shape as the creep zone A_c defined by Riedel and Rice [8] but is six times in size. The latter is the locus of points where the equivalent effective creep strain equals to the equivalent effective elastic strain. As will be shown later in this paper in an example problem, it is found that good agreements can be achieved consistently for a wide range of power-law creep exponents n when A_c' is set to be six times the size of A_c defined by Riedel and Rice [8]. For small scale creep, it can be argued that

$$\int_A W^* dA = \int_{A_c'} W^* dA + \int_{A_e} W^* dA \approx \int_{A_c'} W^* dA \qquad (10)$$

since integration of W^* over the elastic region A_e is negligible compared with the contribution from the creep dominant region A_c'. From equation (10), it can be seen that A_c' has to be larger than Ac because at the boundary of A_e, total creep strains equal to total elastic strains and the W^* values at the boundary of A_e are still not negligible. Also, the net power dissipated in the elastic region is near zero, i. e.,

$$\int_{\partial A} T_i \dot{u}_i\, ds \approx \int_{\partial A_c'} T_i \dot{u}_i\, ds \qquad (11)$$

With equations (10) and (11), $C_o(t)$ defined in equation (4) now reduces to

$$C_o(t) = \frac{d}{da}\left[z\int_{\partial A_c'} T_i \dot{u}_i\, ds - \int_{A_c'} W^*\, dA\right] \qquad (12)$$

where z=1 under load-control conditions and z=0 under displacement-control conditions. It is worth noting that C^* was defined [9] originally under displacement-control conditions while C_t was defined [1] originally under load-control conditions. That is, the P-$\dot{V}$ curves shown in Figure 1 should be constructed by running constant displacement rate tests when measuring C^* but constant load tests when measuring C_t. However, at steady-state creep conditions, both constant load tests and constant displacement rates will lead to the same P-$\dot{V}$ curve due to the

fact that P and $\dot{V}$ at steady-state creep conditions are uniquely related. The same conclusion can not be drawn for C_t at small scale creep or transition creep conditions unless it is for a constant load problem. For a compact-tension specimen with power-law creep under a constant load P, the P-$\dot{V}$ relation [11] has been shown to be,

$$\dot{V}_c = \frac{4\alpha(1-\nu^2)}{E(n-1)} \left(\frac{P}{B}\right)^3 \left(\frac{F^4}{W^2}\right) (EA)^{2/(n-1)}\, t^{-(n-3)/(n-1)} \quad (13)$$

where $\alpha = (1/2\,\pi)[(n+1)^2/1.38n]^{2/(n-1)}$ for $3<n<13$, $A = \dot{\varepsilon}_o/\sigma_o^n$, B is thickness, W is width and F is a K-calibration factor ($F=(K/P)BW^{1/2}$).

Inside the creep dominant zone A_c', the overall strain rate is determined by the power law relationship. Thus, in A_c'

$$W^* = \frac{n}{(n+1)}\, \sigma_{ij}\, \dot{\varepsilon}_{ij} \quad (14)$$

and the stresses, strain rates, and displacements behave asymptotically like the HRR field [8,12,13]:

$$\sigma_{ij} = \sigma_o \left[\frac{C(t)}{\dot{\varepsilon}_o \sigma_o I_n r}\right]^{1/(n+1)} \tilde{\sigma}_{ij}(\theta) \quad (15)$$

$$\dot{\varepsilon}_{ij} = \dot{\varepsilon}_o \left[\frac{C(t)}{\dot{\varepsilon}_o \sigma_o I_n r}\right]^{n/(n+1)} \tilde{\varepsilon}_{ij}(\theta) \quad (16)$$

$$\dot{u}_i = r\dot{\varepsilon}_o \left[\frac{C(t)}{\dot{\varepsilon}_o \sigma_o I_n r}\right]^{n/(n+1)} \tilde{u}_i(\theta) \quad (17)$$

where the dimensionless functions $\tilde{I}_n$, $\tilde{\sigma}_{ij}$, $\tilde{\varepsilon}_{ij}$, *and* $\tilde{u}_i$ have been tabulated by Shih [13] and Symington and Shih [14] for various n values, σ_o is the yield strength, and $\dot{\varepsilon}_o$ is the strain rate at σ_o.

In equation (12), the creep dominant zone A_c' is not fixed in space but is moving and changing in size with different crack lengths, implying that the differentiation procedure used by Rice [6] in deriving J is not applicable here.

We further assumed that the creep zone for the stationary crack of lengths a and $a+\Delta a$ are self similar. That is, it is assumed that

$$r_c(\theta,t) = F(t)\, F_{cr}(\theta) \quad (18)$$

where r_c is radial distance, measured from the crack tip, of the boundary ∂A_c of the creep zone A_c. This assumption is valid as long as the body is under small scale creep. In fact, Riedel and Rice [8] have shown that, under constant loads,

$$r_c(\theta,t) = r_c^o(t)\, F_{cr}(\theta) \quad (19)$$

$$r_c^o(t) = \frac{1}{2\pi} \left(\frac{K}{E}\right)^2 \left[\frac{(n+1)\dot{\varepsilon}_o I_n E^n t}{2\pi(1-\nu^2)\sigma_o^n}\right]^{2/(n-1)} \quad (20)$$

where K is stress intensity factor and $F_{cr}(\theta)$ is a non-dimensional function.

Substituting equations (14) to (17) and applying the differentiation technique described in Appendix A, equation (12) can be reduced to

$$C_{os}(t) = \frac{6}{n+1} F_{cr}\left(\frac{\pi}{2}\right) \left[L_n r_c^o \frac{\partial C(t)}{\partial a} + M_n\, C(t)\, \frac{\partial}{\partial a} r_c^o\right] \quad (21)$$

where the additional subscript "s" on C stands for small scale creep, the factor 6 comes from the assumption that A_c' is six times the size of A_c, and

$$L_n = \frac{1}{I_n} \int_{\partial A_c} \tilde{\sigma}_{ij}\, \tilde{u}_i\, n_j\, d\left[s/r_c\left(\frac{\pi}{2},t\right)\right] \quad (22)$$

$$M_n = \frac{1}{I_n} \int_{\partial A_c} \tilde{\sigma}_{ij}\, \tilde{\varepsilon}_{ij}\, d\left[s/r_c\left(\frac{\pi}{2},t\right)\right] \quad (23)$$

are dimensionless constants which depend on the creep constant n and shape function $F_{cr}(\theta)$ of the creep zone A_c. Under constant load condition, equation (20) can be further simplified as

$$C_{os}(t) = \frac{6}{n+1} F_{cr}\left(\frac{\pi}{2}\right) (L_n + M_n) \frac{K^4(1-\nu^2)}{E^3(n+1)\pi t} \frac{K'}{K} \left[\frac{(n+1) I_n E^n A t}{2\pi(1-\nu^2)}\right]^{2/(n-1)} \quad (24)$$

$$C_{os}(t) = \frac{6}{n+1} F_{cr}\left(\frac{\pi}{2}\right) (L_n + M_n) \frac{k^2(1-\nu^2)}{E(n+1)} \frac{K'}{K} (n-1)\, \dot{r}_c^o \quad (25)$$

where $K' = dK/da$.

Creep zone shapes under mode I loading for different n values have been computed analytically by Riedel and Rice [8]. For the creep zone shapes computed by Riedel and Rice [8], L_n, and M_n for n= 5, 7, 10, 15, and 20 have been calculated and are tabulated along with $F_{cr}\left(\frac{\pi}{2}\right)$ in Table 1. L_n and M_n values listed in Table 1 were calculated based on the $\tilde{\sigma}_{ij}$, $\tilde{\varepsilon}_{ij}$, *and* $\tilde{u}_i$ functions tabulated in References 12 and 13 by Shih and his co-workers. To study the sensitivity of L_n and M_n to the shape of the creep zones, a creep zone shape computed per finite element method by Riedel [14] and an artificially assumed double circle creep zone for n=5 were also used to calculate L_n and M_n, and their results are shown in Table 2. It is seen in this table that $(L_n + M_n)$, which determines C_o, is not very sensitive to the creep zone shapes tested here.

Equations (23) and (24) are very similar to the asymptotic expressions for C_t derived by Saxena [3,10]. From equation (23), it is seen that at small scale creep, $C_o(t)$ (like C_t) is also